

Allosteric modulation of the Lon protease by effector binding and local charges

Justyne L Ogdahl and Peter Chien

University of Massachusetts, Amherst
Department of Biochemistry and Molecular Biology
Molecular and Cellular Biology Program

pchien@umass.edu

1 **Abstract**

2 The ATPase Associated with diverse cellular Activities (AAA+) family of proteases play crucial
3 roles in cellular proteolysis and stress responses. Like other AAA+ proteases, the Lon protease
4 is known to be allosterically regulated by nucleotide and substrate binding. Although it was
5 originally classified as a DNA binding protein, the impact of DNA binding on Lon activity is unclear.
6 In this study, we characterize the regulation of Lon by single-stranded DNA (ssDNA) binding and
7 serendipitously identify general activation strategies for Lon. Upon binding to ssDNA, Lon's ATP
8 hydrolysis rate increases due to improved nucleotide binding, leading to enhanced degradation
9 of protein substrates, including physiologically important targets. We demonstrate that mutations
10 in basic residues that are crucial for Lon's DNA binding not only reduces ssDNA binding but result
11 in charge-specific consequences on Lon activity. Introducing negative charge at these sites
12 induces activation akin to that induced by ssDNA binding, whereas neutralizing the charge
13 reduces Lon's activity. Based on single molecule measurements we find that this change in
14 activity is correlated with changes in Lon oligomerization. Our study provides insights into the
15 complex regulation of the Lon protease driven by electrostatic contributions from either DNA
16 binding or mutations.

17

18

19 **Highlights:**

- 20 • ssDNA binding allosterically activates Lon ATP hydrolysis
- 21 • Negative charge at DNA binding site is sufficient for Lon activation
- 22 • Neutralization of charge at DNA binding site inhibits Lon ATP hydrolysis
- 23 • Lon activity is linked to formation of stable Lon hexamers

24 **Significance:**

25

26 The energy-dependent protease Lon is integral in both eukaryotic and prokaryotic physiology,
27 contributing to protein quality control, stress management, developmental regulation, and
28 pathogenicity. The ability to precisely regulate protein levels through targeted degradation
29 underscores a need for tunability. We find that single-stranded DNA (ssDNA) acts as an allosteric
30 regulator of Lon, leading to enhanced enzymatic activity. Mutations in basic residues crucial for
31 DNA binding were found to affect Lon activity in a charge-specific manner highlighting the
32 importance of electrostatic interactions regulating Lon's function. Changes in Lon activity due to
33 ssDNA binding or mutations were correlated with its oligomerization state. Our findings provide
34 insights into the activation strategies of Lon, emphasizing the role of electrostatic contribution that
35 modulate nucleotide affinity, oligomerization and proteolysis to advance our understanding of the
36 complex regulatory mechanisms of the Lon protease.

37

38
39
40
41
42
43
44
45
46
47
48
49
50
51
52
53
54
55

Introduction:

The ATPase Associated with diverse cellular Activities (AAA+) family of proteases is important for regulated proteolysis in both eukaryotic and prokaryotic cells. Among this family, the Lon protease plays a particular importance in ensuring protein quality control and managing cellular stress response in bacteria (1–4). Because protein degradation is irreversible, there is a pressing need for highly controlled regulation of these proteases to ensure the rapid and specific breakdown of substrates. Most proteases recognize substrates via sequence tags, known as degrons. In the case of the Lon protease, one class of these degrons are peptide motifs rich in hydrophobic residues, supporting a quality control role for the Lon protease in recognizing misfolded or unfolded proteins (5–7). Similar to all other AAA+ proteases, Lon captures the energy of ATP hydrolysis to undergo conformational changes that enable the recognition, unfolding and translocation of proteins into a nonspecific oligomeric peptidase cavity for degradation (8). In addition, Lon is particularly sensitive to allosteric regulation, with strong coupling between activities of each domain and adopting multiple distinct conformational states during the functional cycling of this protease (6,9,10).

56
57
58
59
60
61
62
63
64

The polypeptide product of the *E. coli lon* gene was initially identified as a DNA binding protein, originally designated CapR for its role in regulating capsular synthesis and cell elongation (11–14). The discovery of Lon as an ATP-dependent protease gave rise to considerable speculation on the role of DNA binding for the activity or function of Lon (14–21). Understanding this phenomenon was challenging because of differences in specific preparations and approaches for measuring Lon activity. For example, one study showed that denatured DNA stimulates casein degradation by Lon in an ATP dependent manner, while another demonstrated that addition of DNA limited proteolytic activity (22,23). Our recent studies revealed that in *Caulobacter crescentus* (hereafter referred as *C. crescentus*) Lon is recruited to the chromosome to clear

65 DNA-bound proteins as a part of the genotoxic stress response, a function preserved in
66 mitochondria (24). These varied and conflicting results led us to systematically explore the
67 biochemical consequences of DNA binding for the Lon protease activity, using *C. crescentus* as
68 our model system.

69

70 In this current work, we reveal that although Lon can bind both dsDNA and ssDNA, only ssDNA
71 binding causes changes in Lon biochemical activity. Upon ssDNA binding, ATP hydrolysis of Lon
72 increases primarily due to enhanced affinity for ATP nucleotide and protection from ADP
73 inhibition. This heightened ATP hydrolysis subsequently leads to increased degradation of
74 protein substrates, including known physiologically important targets of Lon. Our findings indicate
75 that mutating basic residues that are essential for binding DNA results in loss of ssDNA binding
76 with charge-specific consequences. Substituting these residues with negatively charged
77 glutamates (Lon4E) induced a similar level of activation as ssDNA binding. However, neutralizing
78 charge at this site (Lon4A) results in a poorly active Lon, compromised for ATP hydrolysis, more
79 prone to inhibition by ADP, but still fully capable of assembling into peptidase-active Lon
80 oligomers when substrate and nucleotide are present. We take advantage of these mutants to
81 show that when Lon is primed to adopt an activated state, formation of the peptidase site requires
82 only binding of ATP, but not hydrolysis, and that activation of Lon is correlated with persistent
83 formation of higher molecular weight species.

84

85 Taken together, our results demonstrate that changes in surface electrostatics, induced by ssDNA
86 binding or mutations at DNA binding sites, can induce formation of a state of Lon that is more
87 readily activated for protein degradation.

88

89

90

91 **Results**

92 **ssDNA activates Lon upon binding.**

93 Although Lon has been known to be a nucleic acid binding protein for some time, the
94 consequences of single stranded DNA binding on Lon activity are unclear, with reports differing
95 on whether it activates or inhibits. We took a biochemical approach to address this question as
96 our previous work suggested that dsDNA could act as a scaffold for protein degradation (24).
97 Interestingly, we found that while dsDNA did not affect Lon activity directly, addition of ssDNA
98 significantly enhanced proteolysis of the model substrate casein (Figure 1A). This proteolytic
99 activation extended to physiologically known Lon substrates, as the regulatory factors DnaA,
100 CcrM and SciP were all degraded more rapidly in the presence of ssDNA (36 base
101 oligonucleotide; OPC698) (Figure 1B, Supplemental Figure S1A). Using a polarization assay to
102 monitor fluorescently labeled ssDNA binding to Lon, we found that ssDNA bound more tightly to
103 Lon than dsDNA (Supplemental Figure S1B). Consistent with the need for ATP hydrolysis to
104 induce degradation, ssDNA increased the intrinsic ATPase activity of Lon, whereas dsDNA did
105 not (Figure 1C). Finally, adding ssDNA increased the peptidase activity of Lon, even without
106 protein substrate (Figure 1D). Because oligomerization is needed to form the peptide hydrolysis
107 site, we hypothesized that ssDNA binding may affect Lon activity through oligomerization, a
108 direction we explore below.

109

110 As mentioned above, early investigations into the effects of DNA binding on Lon activity showed
111 conflicting results, as some indicated that ssDNA activated Lon proteolysis (23), while others
112 showed inhibition (22). In our initial studies, we had used various ssDNA ligands, including
113 oligonucleotides containing G-quadruplex (G4) sequences (30 base oligonucleotide; OPC498
114 and 36 base oligonucleotide OJO19), a known binding motif for Lon (14,15,20). Interestingly, we
115 observed that these G4 oligonucleotides inhibited casein degradation, but still increased

116 stimulation of ATP hydrolysis and peptide hydrolysis (Supplemental Figure S2A, B). Additionally,
117 like the original ssDNA described above, G4 oligonucleotides still enhanced degradation of the
118 physiological Lon substrates DnaA and SciP (Supplemental Figure S2C). We conclude that in
119 general ssDNA can stimulate Lon activity, but some sequences can also block degradation of a
120 subset of substrates. We next sought to explore the basis of this activation.

121

122 **Binding of ssDNA increases Lon's oligomerization and increases affinity for nucleotide.**

123 Lon activity is highly dependent on conformational states dictated by the presence of nucleotide
124 and substrate. Activated Lon, bound to substrate, adopts a right-handed closed-ring spiral
125 hexamer and inactive Lon has been found as an open-ring left-handed spiral (25). Recent
126 structural studies further reveal the existence of intermediate oligomers that may contribute to
127 Lon activity (26,27), supporting a general understanding that Lon adopts multiple conformational
128 states during its activation cycle. Given that ssDNA binding directly activates Lon we hypothesized
129 that ssDNA binding affects Lon oligomerization. To test this, we employed mass photometry to
130 measure single particle masses of Lon alone or Lon bound to ssDNA. Our data best fits a
131 distribution where the non-DNA bound Lon forms 75% LMW and 25% HMW. By contrast, DNA
132 bound Lon shifts to 25% LMW and 75% higher-order active species with each Lon monomer
133 binding to one ssDNA. This is evidenced by a MW shift from 528kDa (Lon hexamer) to 588kDa
134 (Lon hexamer with six 11 kDa ssDNA oligonucleotides) as compared to ssDNA alone (Figure 2A,
135 Supplemental Figure 3).

136

137 To understand the impact of ssDNA binding on Lon activity we systematically used ATP and
138 Michaelis-Menten kinetic experiments to determine which activities of Lon are most affected by
139 ssDNA. First, we used saturating concentrations of ATP and titrated casein concentration while
140 measuring initial degradation rates. We found that ssDNA increased the k_{cat} (as defined by
141 $v_{max}/[Lon_6]$) but did not change the K_M (Figure 2B, Table 1). We next titrated ATP in the presence

142 of saturating concentrations of casein and measured initial rates of ATP hydrolysis. Here, with the
143 addition of ssDNA we saw an increase in the k_{cat} and a decrease in the K_M (Figure 2C, Table 1).
144 Our interpretation of these results is that the primary effect of ssDNA on Lon is in modulating the
145 interaction and/or hydrolysis of ATP. Using the Michaelis-Menten formalism with the k_{on}/k_{off}
146 representing the microscopic rate constants for ATP binding to Lon, we know that $K_M = k_{off} / k_{on} +$
147 $k_{cat} / k_{on} = K_D + k_{cat} / k_{on}$. If we assume that the on rate of ATP is only limited by diffusion, then our
148 results suggest that at a minimum, the binding of ATP to Lon must be tighter with ssDNA present
149 given that k_{cat} increased while K_M decreased with the addition of ssDNA.

150

151 ADP is a high affinity inhibitor of Lon even at saturating concentrations of ATP (28). We reasoned
152 that if Lon is binding ATP tighter with ssDNA, then the Lon-ssDNA complex would be more
153 protected from ADP inhibition. Consistent with this model, when we monitored casein degradation
154 as a readout of Lon activity, we found that addition of ssDNA increased the IC50 for ADP 3-fold
155 (Figure 2D). Together with the Michaelis-Menten experiments we conclude that ssDNA binding
156 activates Lon by promoting a higher-order active species with improved ATP binding and
157 hydrolysis, rather than altered substrate affinity.

158

159 **Mutations in the DNA binding site of Lon alter different enzymatic activities.**

160 To better understand how ssDNA impacts Lon, we explored mutations at the DNA binding sites.
161 We previously showed a Lon variant that was unable to bind to chromosomal DNA but retained
162 biochemical activity resulting in a physiological defect during DNA damage but not during
163 proteotoxic stress (24). The Lon4E mutant consists of four lysine to glutamate mutations modeled
164 from prior studies in *E. coli* (29). Our preliminary characterization found Lon4E failed to bind
165 ssDNA (Supplemental Figure 4) but had enhanced catalytic activity, increased ATP hydrolysis
166 and an improved ability to degrade endogenous native substrates compared to wildtype Lon
167 (Figure 3A, B and C). This data points to either the lysine residues acting to limit Lon activity or

168 that inversion of charge at these sites activates Lon similar to the binding of negatively charged
169 ssDNA.

170

171 To distinguish between these two models of activation, we mutated the same lysine residues to
172 the neutral amino acid alanine (Lon4A). We found that the Lon4A was substantially less active
173 than wildtype for protease activity (Figure 3A and B) and ATP hydrolysis (Figure 3A). Interestingly,
174 Lon4A retained wildtype peptidase activity in the presence of ATP with casein (Figure 3C)
175 demonstrating that this Lon variant could still bind nucleotide and substrate to assemble the active
176 peptide hydrolysis catalytic site. Taken together, these findings favor a model where negative
177 charge accumulating on the surface region of Lon, either by changes of side-chain electrostatics
178 or by binding to ssDNA, results in an allosteric activation of Lon ATP hydrolysis.

179

180 **Negative charged residues at the DNA binding site of Lon increase affinity for ATP**

181 Based on our findings indicating that negative surface charge activates Lon we investigated
182 whether Lon4E recapitulates ssDNA bound Lon activity by employing a series of Michaelis-
183 Menten type experiments using the Lon variants. Negative charges at the DNA binding site
184 induced by mutation, Lon4E, substantially increases the k_{cat} for substrate while the K_M remains
185 relatively unchanged compared to wildtype Lon and the Lon4A while the Lon4A has a reduced
186 k_{cat} (Figure 4A, Table 1). Similar to our ssDNA data, Lon4E has an increased k_{cat} with a decreased
187 K_M for ATP hydrolysis, as compared to Lon4A, suggesting that a negative surface charge
188 increases Lon affinity for ATP (Figure 4B, Table 1).

189

190 Our model proposes that the Lon4E resembles a DNA-bound version of Lon, and if this is true we
191 would expect a similar decrease in ADP inhibition. In support of this, we show Lon4E is less
192 inhibited by ADP with a higher IC_{50} as compared to Lon for both degradation of proteins and
193 peptidase activity (Figure 4C and D). By contrast, Lon4A, is more sensitive to ADP with a lower

194 IC50 compared to Lon4E and wildtype Lon (Figure 4D). Together, these results strengthen our
195 findings that a surface exposed positively charged site is allosterically coupled to ATP binding in
196 Lon.

197

198 **Mutations at the Lon DNA binding site alter oligomerization states.**

199 To further investigate the relationship between nucleotide affinity and Lon activation we next
200 determined how peptide hydrolysis is affected. Like for other AAA+ proteases, ATP hydrolysis is
201 not needed for peptide bond cleavage (16,28,30,31) but formation of the peptide hydrolysis active
202 site requires conformational changes that can be induced with nucleotide and substrate binding
203 (25). We find that all variants of Lon could hydrolyze peptide substrates with similar rates in the
204 presence of ATP and casein (Figure 3C, 5A and Supplemental Figure 5A). Closer examination
205 of the traces revealed a lag phase associated with Lon4A peptidase activity (Figure 5A,
206 Supplemental Figure 5A,C), suggestive of a need for some assembly process required prior to
207 the activation of the peptidase active site, likely associated with the slow ATP hydrolysis of Lon4A.
208 To separate the role of ATP hydrolysis from binding, we made use of the poorly hydrolyzed ATP
209 analog AMP-PNP, which can stimulate peptidase activity for *E. coli* Lon (28,32). AMP-PNP alone
210 could stimulate peptide hydrolysis with Lon4E but not wildtype Lon or Lon4A (Supplemental
211 Figure 5B). These results suggest that the different Lon alleles may adopt different populations
212 of conformations reflected by changes in peptide hydrolysis activity, which we sought to clarify
213 with single molecule measurements.

214

215 Upon immediate dilution from concentrated stocks in the absence of nucleotide, wildtype Lon
216 forms high molecular weight (HMW) species (>300 kDa) that are consistent with tetramer to
217 hexamer sized complexes but primarily settles into a lower molecular species (LMW; <200 kDa)
218 consistent with monomers to dimers (Figure 5B). By contrast, Lon4E stays in a HMW species,
219 while the Lon4A is predominantly LMW (Figure 5B). Addition of ATP results in rapid HMW

220 formation for wildtype Lon, but Lon4A remains in a LMW species while Lon4E maintains a HMW
221 profile.

222

223 Our interpretation is that Lon adopts different conformations dependent on allele type which
224 correlates with activation ability. This is particularly interesting as the sites that influence activity
225 in this study are far removed from the oligomeric interfaces seen by structural studies, suggesting
226 an allosteric mechanism linking these activities. The more active Lon4E persists in a dynamic
227 range of larger oligomeric forms while Lon4A readily shifts to a monomeric/dimeric species and
228 fails to assemble higher order oligomers as easily in the presence of nucleotide. Together, these
229 results are consistent with stable hexameric species being the primary enzyme active state of Lon
230 and destabilization observed when Lon cycles to an inactive state such as seen with Lon4A.

231

232 ***In vivo* characterization of Lon alleles**

233 Finally, we tested whether these biochemical differences in Lon activity had any *in vivo*
234 consequences under standard laboratory conditions. We generated strains carrying wildtype,
235 Lon4E or Lon4A alleles as the sole copies of the *lon* gene. All strains grew normally under
236 standard laboratory conditions with all of them rescuing the extended lag phase seen with Δlon
237 strains (Figure 6A). Consistent with the importance of chromosomal binding of Lon in the
238 genotoxic stress pathway (24), both Lon4A and Lon4E were sensitive to DNA damage (Figure
239 6A). All strains were equally resistant to proteotoxic stress generated by misincorporation of
240 canavanine (Figure 6A). Similarly, all strains showed the same ability to degrade DnaA, a known
241 Lon substrate, as determined by translational shut off experiments (Figure 6B). All strains were
242 morphologically similar with respect to cell length, but both DNA-binding deficient Lon alleles
243 result in longer stalk lengths than wildtype cells (Figure 6C, Supplemental Figure 6). Given the
244 dramatic consequences of loss of Lon, these relatively mild effects from Lon alleles suggest that
245 the biochemical differences we observe *in vitro* are bypassed successfully by other features

246 important for *in vivo* activity under laboratory growth conditions, which we discuss in more detail
247 below.

248

249 **Discussion:**

250 The Lon protease is a broadly conserved AAA+ protease found in all kingdoms of life. Lon's
251 activity is encoded on a single polypeptide with functional domains for protein recognition, ATP
252 hydrolysis and peptidase activity. Mechanistically, the complex allosteric control of Lon is likely
253 to stem in part from this linked organization of domains. Physiologically, the fact that Lon
254 recognizes regions of high hydrophobicity rather than sequence-specific degrons allows it to
255 function as a general protein quality protease and justifies the requirement for tight regulation to
256 ensure that unregulated degradation does not harm the cell.

257

258 Although Lon was originally characterized as a DNA binding ATPase, the role of DNA binding for
259 the enzymatic activity of the protease is not clear. In previous studies some reports observed that
260 DNA can stimulate proteolysis of casein by Lon (23) while others report that DNA inhibits
261 proteolysis by the Lon protein without affecting the ATPase activity (22). These apparent
262 discrepancies may be explained by the specific sequences of DNA and the protease substrates
263 used in these past studies. Our work shows that ATP hydrolysis is activated by ssDNA, but we
264 found that G-quadruplex containing ssDNA can also inhibit degradation of unfolded artificial
265 substrates such as casein. We interpret this to mean that although ssDNA can generally activate
266 ATP hydrolysis, and thus degradation of native protein substrates, certain sequences also limit
267 the ability of Lon to degrade unfolded substrates. It is tempting to speculate that this may
268 represent the need for Lon to balance protein quality control (where misfolded protein degradation
269 is important) with the need to degrade regulatory proteins (such as DnaA and CcrM). Additional
270 work is needed to determine if this is true. Finally, studies in mitochondria and bacteria, including
271 that from our own lab (24), have shown that Lon binding to DNA can facilitate degradation of DNA

272 bound proteins. We have shown that this failure to bind DNA is particularly important during
273 genotoxic stress (24) but may also be important for normal physiology, such as degrading the
274 StaR repressor protein (37), which could lead to the stalk length phenotype seen in strains
275 carrying either DNA-binding mutant alleles (Supplemental Figure 6).

276

277 Based on prior studies and our current findings, we propose some additional features of Lon
278 activation. First, Lon binding to single-stranded DNA generally causes an increase in ATP
279 hydrolysis due to an increased affinity of Lon for ATP. Because increased ATP consumption
280 generally leads to increased protein substrate degradation, ssDNA-bound Lon thus degrades
281 proteins faster, but this activation does not change the overall affinity or preference of Lon for its
282 protein substrates. The activated form of Lon protease is less susceptible to inhibition by ADP,
283 suggesting that either ADP binds more poorly by activated Lon or that ATP binds more tightly.
284 Our kinetic data support the latter hypothesis.

285

286 Second, activation of Lon can also arise from introduction of local negative charge at the DNA-
287 binding residues of Lon (Figure 7A), with the same effects on ATP binding and substrate
288 degradation as with ssDNA binding. Neutralization of these charges results in a Lon variant that
289 takes more time to assemble into a peptidase active oligomer, has reduced ATP hydrolysis, and
290 with ATP-alone, fails to readily form oligomers (Figure 7B). We conclude that electrostatic
291 changes introduced by mutation or by ssDNA binding at specific regions that are distant from
292 known protomer-protomer interfaces can shift oligomeric conformations of Lon; satisfying the
293 action-at-a-distance definition of allostery (Figure 7A). Importantly, addition of ssDNA cannot
294 act to simply tether subunits of Lon to promote oligomerization as point mutants have the same
295 activating effects. Finally, we note that other allosteric effectors may bind to this same surface
296 site to elicit changes in Lon activity.

297

298 Despite the clear biochemical differences, we do not see any substantial fitness defects or
299 advantages when comparing strains expressing Lon variants in any laboratory conditions tested
300 so far. One reason for this could be that crowding conditions or substrate concentrations *in vivo*
301 are sufficiently high to promote oligomerization even with the 'inactive' variants. Another may be
302 that under the growth conditions we are studying, even the 5-10% of Lon activity sustained by the
303 'inactive' variant *in vitro* may be sufficient for physiological need or stress response. Given the
304 biochemical differences, it is tempting to speculate that other conditions may reveal more
305 physiological impact, such as during changes in ADP/ATP ratios during nutrient starvation. Due
306 to the importance of Lon as a quality control protease and as a cell cycle regulator it is also
307 possible that Lon utilizes other regulatory mechanisms, such as the upregulation of the Lon
308 activator LarA during proteotoxic stress (4) or other regulators, yet to be determined, in order to
309 maintain proteostasis. The *in vivo* consequences of Lon activation are a fascinating topic for future
310 studies.

311
312 Collectively, our findings point to a complex allosteric landscape of Lon that connects
313 oligomerization state, ligand binding, local electrostatics, and enzyme activity. Given the
314 pleiotropic impact of Lon in every system where it has been studied, we predict that accounting
315 for this complex regulation may be important for understanding the general role of this quality
316 control protease.

317

318

319 **Methods**

320

321 **Cloning, Protein expression and purification**

322

323 Protein purification

324 *Caulobacter* pBAD33-Lon, pBAD33-Lon4E and pBAD33-Lon4A were purified as previously
325 described, using hydroxyapatite resin (Sigma Aldrich) and ion exchange (MonoQ)
326 chromatography. His₆SciP and His₆CcrM were purified as previously described (38). DnaA was
327 purified (39) by expressing His₆ tagged SUMO-DnaA fusion construct and using a Ni-NTA-
328 agarose resin, removal of the SUMO tag by Ulp1 proteolytic cleavage and a reverse Ni-NTA. Ion
329 exchange (MonoS) chromatography using S-buffer 100mM KCl (25mM HEPES PH7.5, 200mM
330 L-Glutamic acid potassium, 10mM MgCl₂ and 1mM DTT) and elution buffer containing 1M KCl
331 (25mM HEPES PH7.5, 200mM L-Glutamic acid potassium, 300mM Imidazole, 10mM MgCl₂ and
332 1mM DTT).

333

334 Construct design and Cloning.

335 pBAD33-Lon4A was constructed using the pBAD33-Lon as a template. 4A mutations were made
336 via site directed mutagenesis PCR and sequence validated (Plasmidsaurus). Lon deletion strains
337 and Lon4E cell lines were constructed as previously described (24), using the pNPTS138 plasmid.
338 Allelic replacement of Lon4A was performed by transforming the pNPTS138-Lon4A into
339 lon::specR cell line with primary selection on PYE with kanamycin (25ug/mL) and secondary
340 selection on PYE with 3%(w/v) sucrose. Clonal lines were confirmed by antibiotic sensitivity and
341 using whole genome sequencing (SeqCenter, Pittsburgh,PA).

342

343 ***In vitro* assays**

344

345 Dual *In vitro* protein degradation and ATPase assay

346 Lon degradation and ATPase assays for all alleles, unless noted, were performed at 30°C in a
347 Lon activity buffer [50mM TRIS pH 8.00 10mM MgCl, 100mM KCL]. Lon alleles were used at
348 0.1uM Lon₆, 125ng/mL FITC-casein Type II (dissolved in water and stored at -80C) (Sigma
349 Aldrich), 2mM ATP, 1mM phosphoenolpyruvate, 10U/mL pyruvate kinase, 30U/mL lactate
350 dehydrogenase and 0.4mM NADH (Sigma Aldrich) with or without 20μM ssDNA. Degradation and
351 ATP hydrolysis reactions were monitored in a dual assay on a SpectraMaxM2 (Molecular
352 Devices) in a 384 non-binding black well plate (Corning). Proteolysis was determined by an
353 increase of fluorescence by the unquenched FITC fluorophore at the following wavelengths,
354 Ex465nm-Em520nm. ATPase was monitored using wavelengths at Ex340nm-Em470nm by a
355 coupled NADH- fluorescence assay where oxidation of NADH corresponds to 1:1 with ATP
356 hydrolyzed. Rates of the reaction were determined by: FITC-casein degraded ($\text{min}^{-1} \text{Lon}_6^{-1}$) used
357 the V_{max} of slope/min at steady state/ $9.5/26/1000/[\text{Lon}_6 \text{ allele}]$. ATP hydrolysis used the V_{max} of
358 slope/min at steady state/ $-1/2361/[\text{Lon}_6 \text{ allele}]$. Degradation and ATP hydrolysis rates were fit to
359 a modified non-linear regression model.

360 *In vitro* proteolysis assay

361 Each *in vitro* proteolysis assay was performed in Lon activity buffer (described in the dual *in vitro*
362 assays) and an ATP regeneration mix [4mM ATP, 75 ng/mL creatine kinase and 5mM creatine
363 phosphate] (Sigma). Lon₆ and substrate concentrations are indicated in figure legends. Samples
364 were preincubated at 30°C and the reactions were initiated by the addition of ATP regeneration
365 mix. Time points taken as specified in the figure legend and concentrations were normalized with
366 2X SDS-loading dye and flash frozen. Samples were run on 10% (unless otherwise specified)
367 polyacrylamide SDS-Page gels and stained with Coomassie.

368 Fluorescent Polarization assay

369 Purified protein was incubated at 30°C in the following buffer with 25mM Hepes pH7.5, 10 mM
370 MgCl, 100mM KCl and 0.05% TWEEN-20. Lon alleles were used at 0.1μM (all concentrations in
371 hexamer), 25nM DNA labeled with fluorescein (FAM) (Integrated DNA Technologies), 25nM

372 ssDNA (OPC698) and 25nM dsDNA G1Box (24) oligonucleotides annealed (Integrated DNA
373 Technologies). Polarization was measured on a SpectraMaxM5 microplate reader (Molecular
374 Devices) at excitation and emission wavelengths at 460nm-540nm with 530nm cutoff.

375 Peptidase Activity

376 Peptidase assays were performed using Lon activity buffer, 125 nM Glutaryl-Ala-Ala-Phe-4-
377 methyl- β -naphthylamide (Sigma-Aldrich), 0.1 μ M Lon₆, 125 ng/mL casein (Thermo Fisher
378 Scientific) and an ATP regeneration mix [4 mM ATP, 75 ng/mL creatine kinase and 5 mM creatine
379 phosphate]. Peptide hydrolysis was evaluated as an increase in fluorescence on a SpectraMaxM2
380 (Molecular Devices) at excitation and emission wavelengths 335nm-410nm.

381 Mass Photometry

382 Mass photometry experiments were carried out using OneMP mass photometer (Refeyn LTD,
383 Oxford, UK) at room temperature with Aquire MP software for data analysis. Experimental
384 procedure setup was performed as previously described (40). Proteins variants were diluted to
385 200 nM monomeric final concentrations in 25mM TRIS PH 8.0, 10mM MgCl, 100mM KCl, 1mM
386 TCEP and imaged immediately after dilution, 10', 15', and post ATP addition (1mM). Experiments
387 were done in triplicate at different times.

388 ***In vivo* assays**

389

390 Bacterial strains and growth conditions

391 All *Caulobacter crescentus* cells used in this study originated from the NA1000 strain. Liquid
392 cultures of *Caulobacter* were grown at 30°C in a peptone yeast extract (PYE) medium containing
393 2g/L Peptone, 1g/L yeast, 1mM MgSO₄ and 0.5mM CaCl₂. Solid media conditions were grown at
394 30C on PYE with 1.5% bacto-agar. *E. coli* cells were grown in either liquid or solid media (1.5%
395 agar) at 37°C in lysogeny broth (LB). Cell strains (see construct design and cloning) were cultured
396 using antibiotics at the following concentrations: Kanamycin 50 μ g/mL, Chloramphenicol 30
397 μ g/mL, Tetracycline 15 μ g/mL L, Spectinomycin 100 μ g/mL.

398 *In vivo* proteolysis Assays

399 Protein stability *in vivo* was monitored by translational shut offs using 30 ug/mL of
400 chloramphenicol added to exponentially growing cells (OD₆₀₀ 0.4-0.6). At each time point specified
401 1mL of cells was removed, centrifuged for 5' at 6000Xg and normalized by OD₆₀₀ using 2X SDS
402 loading dye and flash frozen. Pellets were boiled for 10min and centrifuged at 21000xg for 10'.
403 Each sample was loaded onto a 10% Bis-TRIS SDS/Page gel and run at 150V for 1 hour and
404 transferred to a nitrocellulose membrane (Cytiva). Membranes were blocked for 1 hour at room
405 temp with 5% milk in 1X TBST (20mM TRIS and 150mM NaCl with 0.1% TWEEN-20) and primary
406 antibodies were used with 5% milk in 1X TBST at 4°C overnight using the following
407 dilutions:1:5000 anti-DnaA, 1:10000 anti-ClpP, 1:5000 anti-Lon. Membranes were washed 3x 5'
408 1X TBST at room temp,1:15000 IRdye800 goat anti-rabbit secondary (Li-COR) in 5% milk in 1X
409 TBST 1 hour at room temp and washed 3x 1X TBST and imaged using the Li-COR Odyssey
410 scanner. Densitometry for degradation was determined using Fiji(41) (NIH) and plotted using
411 Prism (Graph Pad).

412 **Bacterial Characterization: Morphology, viability, and stress Assays**

413 Cultures were diluted to OD₆₀₀ 0.05 and grown to OD₆₀₀ 0.5. Morphological characterization of
414 cells was done using phase contrast microscopy (Zeiss AXIO ScopeA1). Cells were mounted
415 onto 1% agarose-PYE pads and imaged under 100X oil immersion. Stalks were measured by
416 Fiji(41) (NIH) and cell length was measured by MicrobeJ for ImageJ (42). Growth curves were
417 performed by plate reader at 30C with PYE, 0.25-0.5µg/mL Mitomycin C (MMC), 100µg/mL L-
418 Canavanine and monitored using OD₆₀₀.

419 Quantification and statistical analysis

420 Graphs were generated by Prism (GraphPad). Error bars represent SD n=3 and the 95%CI is
421 reported. To determine kinetic parameters of proteolysis (r_{deg}) (Eq1) and ATP hydrolysis (r_{ATPase})
422 (Eq2) of Lon for [substrate] or [ATP] we employed non-linear regression with a hill coefficient via

423 an allosteric sigmoidal model. V_{max} is the maximum enzyme velocity, K_M is the Michaelis-Menten
424 equation in the same units as [substrate], n is the hill slope =>0.

$$425 \quad r_{deg} = V_{max} * \frac{[FITC-Casein]^n}{(K_m^n + [FITC-Casein]^n)} \quad Eq1.$$

$$426 \quad r_{ATPase} = V_{max} * \frac{[ATP]^n}{(K_m^n + [ATP]^n)} \quad Eq2.$$

427

428 To determine the IC_{50} for ADP, data was normalized and fit using a [inhibitor] vs normalized
429 response with variable slope model (Eq3) with the equation:

$$430 \quad \text{Normalized response} = \frac{100}{(1 + (IC_{50}/[ADP])^{HillSlope})} \quad Eq3.$$

431

432 **Acknowledgments**

433 We thank all members of the Chien lab for comments. Special thanks to Rilee Zeinert for
434 discussion. Funding was provided for in part from NIH T32 GM235096 (JLO) and NIGMS R35
435 GM130320 (PC).

436

437
438
439
440
441
442
443
444
445
446
447
448
449
450
451
452
453
454
455
456
457
458
459
460
461
462
463
464
465
466
467
468
469
470
471
472

Citations

1. A. Konovalova, L. Søggaard-Andersen, L. Kroos, Regulated proteolysis in bacterial development. *FEMS Microbiol. Rev.* **38**, 493–522 (2014).
2. S. A. Mahmoud, P. Chien, Regulated Proteolysis in Bacteria. *Annu. Rev. Biochem.* **87**, 677–696 (2018).
3. Akar Roy, Fink Matthias J., Omnus Deike J., Jonas Kristina, Regulation of the general stress response sigma factor σ^T by Lon-mediated proteolysis. *J. Bacteriol.* **205**, e00228-23 (2023).
4. D. J. Omnus, *et al.*, The heat shock protein LarA activates the Lon protease in response to proteotoxic stress. *Nat. Commun.* **14**, 7636 (2023).
5. L. Waxman, A. L. Goldberg, Selectivity of Intracellular Proteolysis: Protein Substrates Activate the ATP-Dependent Protease (La). *Science* **232**, 500–503 (1986).
6. E. Gur, R. T. Sauer, Degrons in protein substrates program the speed and operating efficiency of the AAA+ Lon proteolytic machine. *Proc. Natl. Acad. Sci. U. S. A.* **106**, 18503–18508 (2009).
7. K. Jonas, J. Liu, P. Chien, M. T. Laub, Proteotoxic Stress Induces a Cell-Cycle Arrest by Stimulating Lon to Degrade the Replication Initiator DnaA. *Cell* **154**, 623–636 (2013).
8. R. T. Sauer, T. A. Baker, AAA+ Proteases: ATP-Fueled Machines of Protein Destruction. *Annu. Rev. Biochem.* **80**, 587–612 (2011).
9. E. Gur, “The Lon AAA+ Protease” in *Regulated Proteolysis in Microorganisms*, D. A. Dougan, Ed. (Springer Netherlands, 2013), pp. 35–51.
10. N. Puri, A. W. Karzai, HspQ Functions as a Unique Specificity-Enhancing Factor for the AAA+ Lon Protease. *Mol. Cell* **66**, 672-683.e4 (2017).
11. P. Howard-Flanders, E. Simson, L. Theriot, A locus that controls filament formation and sensitivity to radiation in *Escherichia coli* k-12. *Genetics* **49**, 237–246 (1964).
12. Adler Howard I., Hardigree Alice A., Analysis of a gene controlling cell division and sensitivity to radiation in *Escherichia coli*. *J. Bacteriol.* **87**, 720–726 (1964).
13. B. A. Zehnbaauer, E. C. Foley, G. W. Henderson, A. Markovitz, Identification and purification of the Lon+ (*capR*+) gene product, a DNA-binding protein. *Proc. Natl. Acad. Sci. U. S. A.* **78**, 2043–2047 (1981).
14. G. K. Fu, M. J. Smith, D. M. Markovitz, Bacterial Protease Lon Is a Site-specific DNA-binding Protein *. *J. Biol. Chem.* **272**, 534–538 (1997).
15. G. K. Fu, D. M. Markovitz, The Human LON Protease Binds to Mitochondrial Promoters in a Single-Stranded, Site-Specific, Strand-Specific Manner. *Biochemistry* **37**, 1905–1909 (1998).

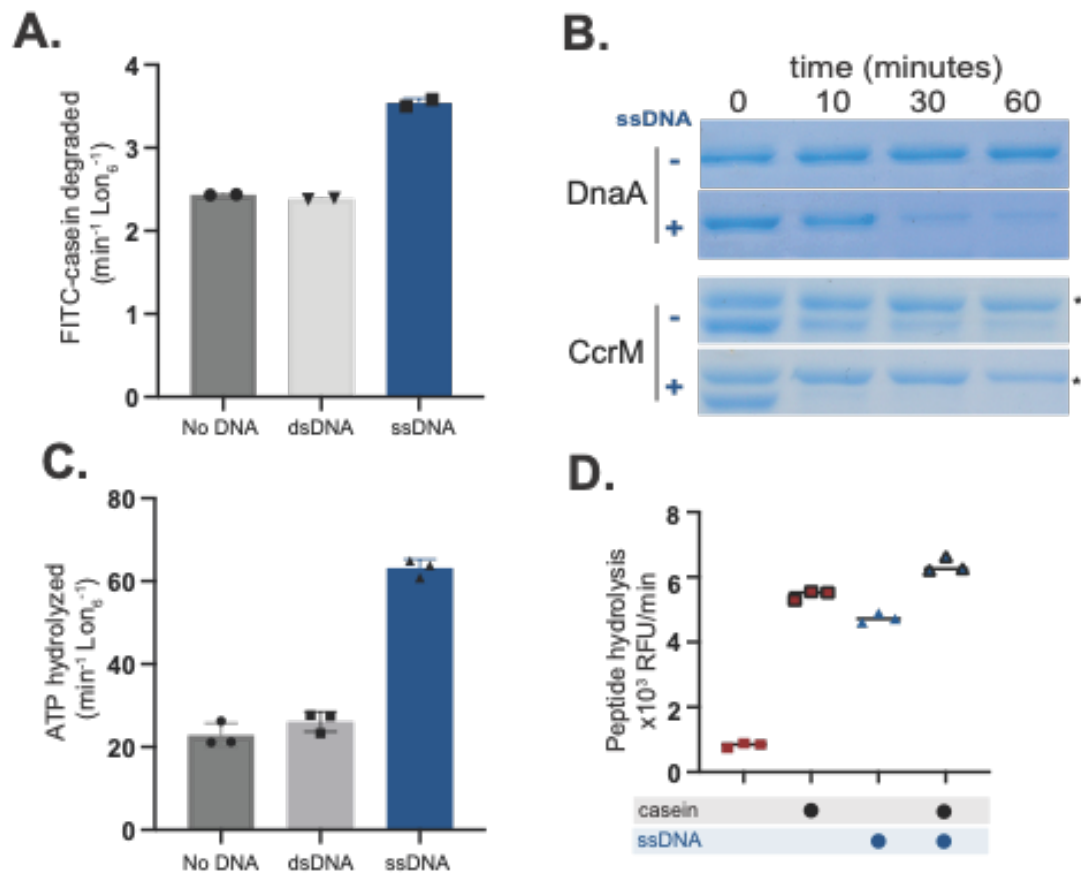
- 473 16. I. Lee, C. K. Suzuki, Functional mechanics of the ATP-dependent Lon protease- lessons
474 from endogenous protein and synthetic peptide substrates. *Biochim. Biophys. Acta* **1784**,
475 727–735 (2008).
- 476 17. A. Y.-L. Lee, C.-H. Hsu, S.-H. Wu, Functional Domains of *Brevibacillus thermoruber* Lon
477 Protease for Oligomerization and DNA Binding: Role of N-terminal and sensor and substrate
478 Discrimination domains . *J. Biol. Chem.* **279**, 34903–34912 (2004).
- 479 18. A. Y.-L. Lee, *et al.*, Structural basis for DNA-mediated allosteric regulation facilitated by the
480 AAA⁺ module of Lon protease. *Acta Crystallogr. D Biol. Crystallogr.* **70** (2014).
- 481 19. B. Lu, *et al.*, Roles for the human ATP-dependent Lon protease in mitochondrial DNA
482 maintenance. *J. Biol. Chem.* **282**, 17363–17374 (2007).
- 483 20. B. Lu, *et al.*, The ATP-dependent Lon protease of *Mus musculus* is a DNA-binding protein
484 that is functionally conserved between yeast and mammals. *Gene* **306**, 45–55 (2003).
- 485 21. B. Lu, *et al.*, Phosphorylation of human TFAM in mitochondria impairs DNA binding and
486 promotes degradation by the AAA⁺ Lon protease. *Mol. Cell* **49**, 121–132 (2013).
- 487 22. M. F. Charette, G. W. Henderson, L. L. Doane, A. Markovitz, DNA-stimulated ATPase
488 activity on the lon (CapR) protein. *J. Bacteriol.* **158**, 195–201 (1984).
- 489 23. C. H. Chung, A. L. Goldberg, DNA stimulates ATP-dependent proteolysis and protein-
490 dependent ATPase activity of protease La from *Escherichia coli*. *Proc. Natl. Acad. Sci. U. S.*
491 *A.* **79**, 795–799 (1982).
- 492 24. R. D. Zeinert, *et al.*, “A legacy role for DNA binding of Lon protects against genotoxic stress”
493 (Microbiology, 2023).
- 494 25. M. Shin, *et al.*, Structural basis for distinct operational modes and protease activation in
495 AAA⁺ protease Lon. *Sci. Adv.* **6**, (2020).
- 496 26. I. Botos, *et al.*, Cryo-EM structure of substrate-free *E. coli* Lon protease provides insights
497 into the dynamics of Lon machinery. *Curr. Res. Struct. Biol.* **1**, 13–20 (2019).
- 498 27. S. Li, *et al.*, A 5+1 assemble-to-activate mechanism of the Lon proteolytic machine. *Nat.*
499 *Commun.* **14**, 7340 (2023).
- 500 28. J. Thomas-Wohlever, I. Lee, Kinetic Characterization of the Peptidase Activity of *Escherichia*
501 *coli* Lon Reveals the Mechanistic Similarities in ATP-Dependent Hydrolysis of Peptide and
502 Protein Substrates. *Biochemistry* **41**, 9418–9425 (2002).
- 503 29. A. Karlowicz, *et al.*, Defining the crucial domain and amino acid residues in bacterial Lon
504 protease for DNA binding and processing of DNA-interacting substrates. *J. Biol. Chem.* **292**,
505 7507–7518 (2017).
- 506 30. D. Vineyard, J. Patterson-Ward, A. J. Berdis, I. Lee, Monitoring the Timing of ATP Hydrolysis
507 with Activation of Peptide Cleavage in *Escherichia coli* Lon by Transient Kinetics.
508 *Biochemistry* **44**, 1671–1682 (2005).

- 509 31. I. Lee, A. J. Berdis, Adenosine Triphosphate-Dependent Degradation of a Fluorescent λ N
510 Substrate Mimic by Lon Protease. *Anal. Biochem.* **291**, 74–83 (2001).
- 511 32. M. R. Maurizi, Degradation in vitro of bacteriophage lambda N protein by Lon protease from
512 Escherichia coli. *J. Biol. Chem.* **262**, 2696–2703 (1987).
- 513 33. Y. Matsushima, Y. Goto, L. S. Kaguni, Mitochondrial Lon protease regulates mitochondrial
514 DNA copy number and transcription by selective degradation of mitochondrial transcription
515 factor A (TFAM). *Proc. Natl. Acad. Sci.* **107**, 18410–18415 (2010).
- 516 34. T. Liu, *et al.*, DNA and RNA Binding by the Mitochondrial Lon Protease Is Regulated by
517 Nucleotide and Protein Substrate. *J. Biol. Chem.* **279**, 13902–13910 (2004).
- 518 35. N. Kunová, *et al.*, The role of Lon-mediated proteolysis in the dynamics of mitochondrial
519 nucleic acid-protein complexes. *Sci. Rep.* **7**, 631 (2017).
- 520 36. Y.-C. Lin, *et al.*, DNA-binding specificity of the Lon protease α -domain from *Brevibacillus*
521 *thermoruber* WR-249. *Biochem. Biophys. Res. Commun.* **388**, 62–66 (2009).
- 522 37. D. J. Omnus, M. J. Fink, K. Szewo, K. Jonas, The Lon protease temporally restricts polar
523 cell differentiation events during the *Caulobacter* cell cycle. *eLife* **10**, e73875 (2021).
- 524 38. K. G. Gora, *et al.*, Regulated proteolysis of a transcription factor complex is critical to cell
525 cycle progression in *Caulobacter crescentus*. *Mol. Microbiol.* **87**, 1277–1289 (2013).
- 526 39. K. Jonas, J. Liu, P. Chien, M. T. Laub, Proteotoxic Stress Induces a Cell-Cycle Arrest by
527 Stimulating Lon to Degrade the Replication Initiator DnaA. *Cell* **154**, 623–636 (2013).
- 528 40. A. P. Torres-Ocampo, *et al.*, Characterization of CaMKII α holoenzyme stability. *Protein Sci.*
529 *Publ. Protein Soc.* **29**, 1524–1534 (2020).
- 530 41. J. Schindelin, *et al.*, Fiji: an open-source platform for biological-image analysis. *Nat.*
531 *Methods* **9**, 676–682 (2012).
- 532 42. A. Ducret, E. M. Quardokus, Y. V. Brun, MicrobeJ, a tool for high throughput bacterial cell
533 detection and quantitative analysis. *Nat. Microbiol.* **1**, 16077 (2016).

534
535

536

Figure 1



537
538
539
540
541
542
543
544
545
546
547
548

Figure 1. Lon binding to ssDNA increases activity. A. *In vitro* proteolysis of FITC-Casein comparing activation of purified Lon with ssDNA and dsDNA. B. Gel based *in vitro* degradation of the purified Lon substrates, DnaA (5 μ M) and CcrM (5 μ M) with and without ssDNA. Creatine kinase (*) is a component of the ATP regeneration mix. C. Basal ATPase activity with DNA using an *in vitro* ATP hydrolysis assay. D. Lon peptidase activity was obtained using the fluorogenic peptide (Glut-Ala-Ala-Phe-MNA) with and without Casein and DNA and an ATP regeneration mix with creatine kinase and creatine phosphate. All assays were performed using 0.1 μ M Lon₆, 2mM ATP and 20 μ M DNA when noted.

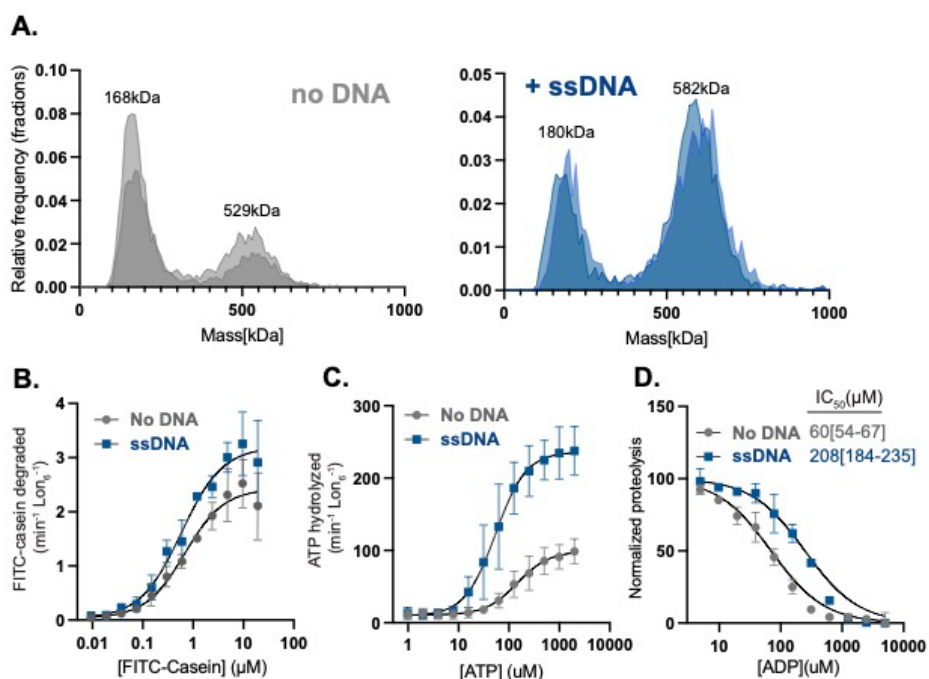
549
 550 **Table 1.** Steady state kinetic parameters of proteolysis and ATP hydrolysis with Lon variants and
 551 ssDNA derived from a modified allosteric sigmoidal model with the 95%CI (asymptotic) shown.

Lon variant	Casein Degradation			ATP Hydrolysis		
	K_M (μM)	k_{cat} ($\text{min}^{-1}\text{Lon}^{-1}$)	Hill constant	K_M (μM)	k_{cat} ($\text{min}^{-1}\text{Lon}^{-1}$)	Hill constant
Lon	0.7[0.6-0.9]	2.0[1.5-2.9]	1.1[0.5-1.7]	92[67-135]	88[77-103]	1.2[0.8-1.8]
Lon/ssDNA	0.6[0.3-0.9]	3.2[2.5-3.8]	1.1[0.5-1.6]	54 [40-74]	226 [201-257]	1.4[1-2]
Lon4E	1.0[0.8-1.5]	4.0[3.6-4.3]	1.9[1.6-2.4]	28[23-28]	272[246-301]	1.6[1.2-2.3]
Lon4A	0.9[0.5-1.7]	0.2[0.1-0.2]	2.0[1.2-4]	206[134-707]	45[36-75]	1.2[0.7-1.8]

552
 553

554

Figure 2



555

556

557

558 **Figure 2 Binding of ssDNA increases oligomerization and Lon's affinity for nucleotide. A.**

559 Mass photometry measurements of Lon with (or without ssDNA (shaded colors represent two

560 biological replicates). B. Michaelis-Menten plot showing the rate of degradation as a function of

561 the concentration of FITC-Casein with and without ssDNA. C. The rate of ATP hydrolysis as a

562 function of the concentration of ATP with 1.2 μM FITC-Casein. D. FITC-Casein degradation

563 normalized as a function of the concentration of ADP by Lon with and without ssDNA. MP

564 experiments used 200 nM Lon monomer concentration. All other assays were performed using

565 an ATP regeneration system with 0.1 μM Lon₆, 20 μM ssDNA and 125 $\mu\text{g}/\text{mL}$ FITC-casein with

566 the exception or the ADP titration which did not use an ATP regeneration mix but instead used

567 1mM ATP to initiate the reaction.

568

569

570

571

572

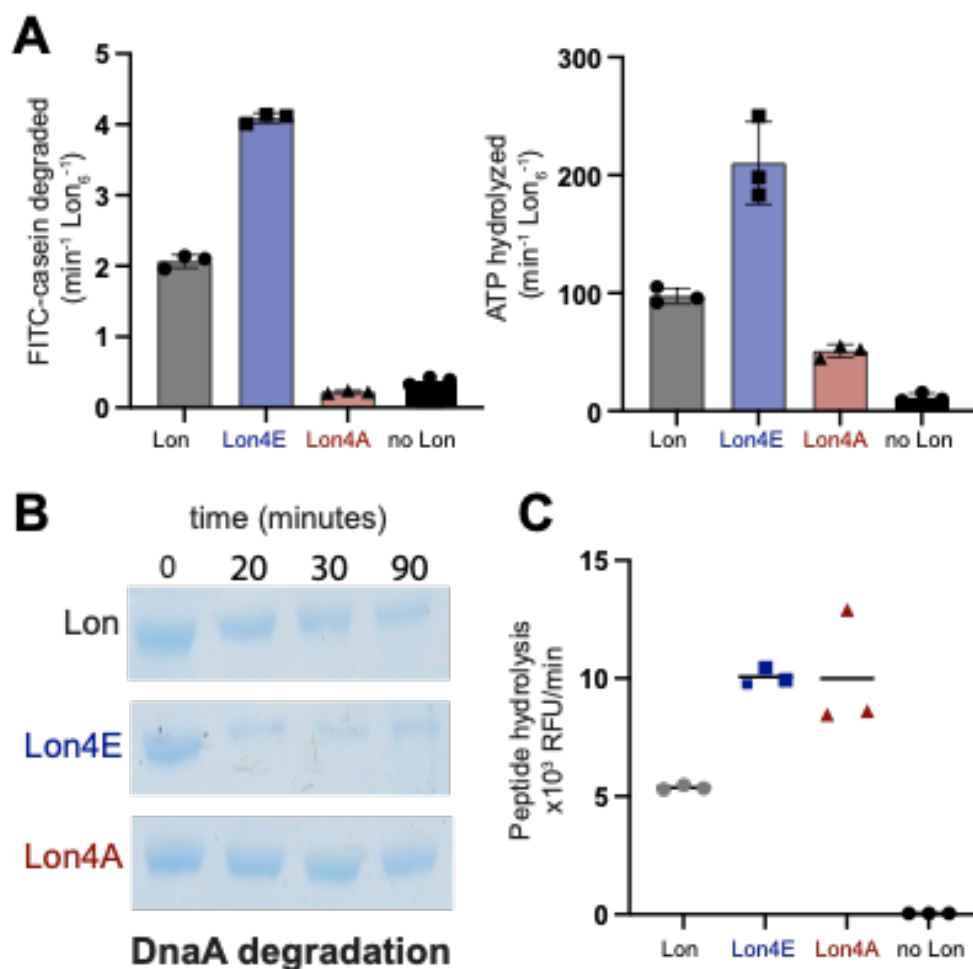
573

574

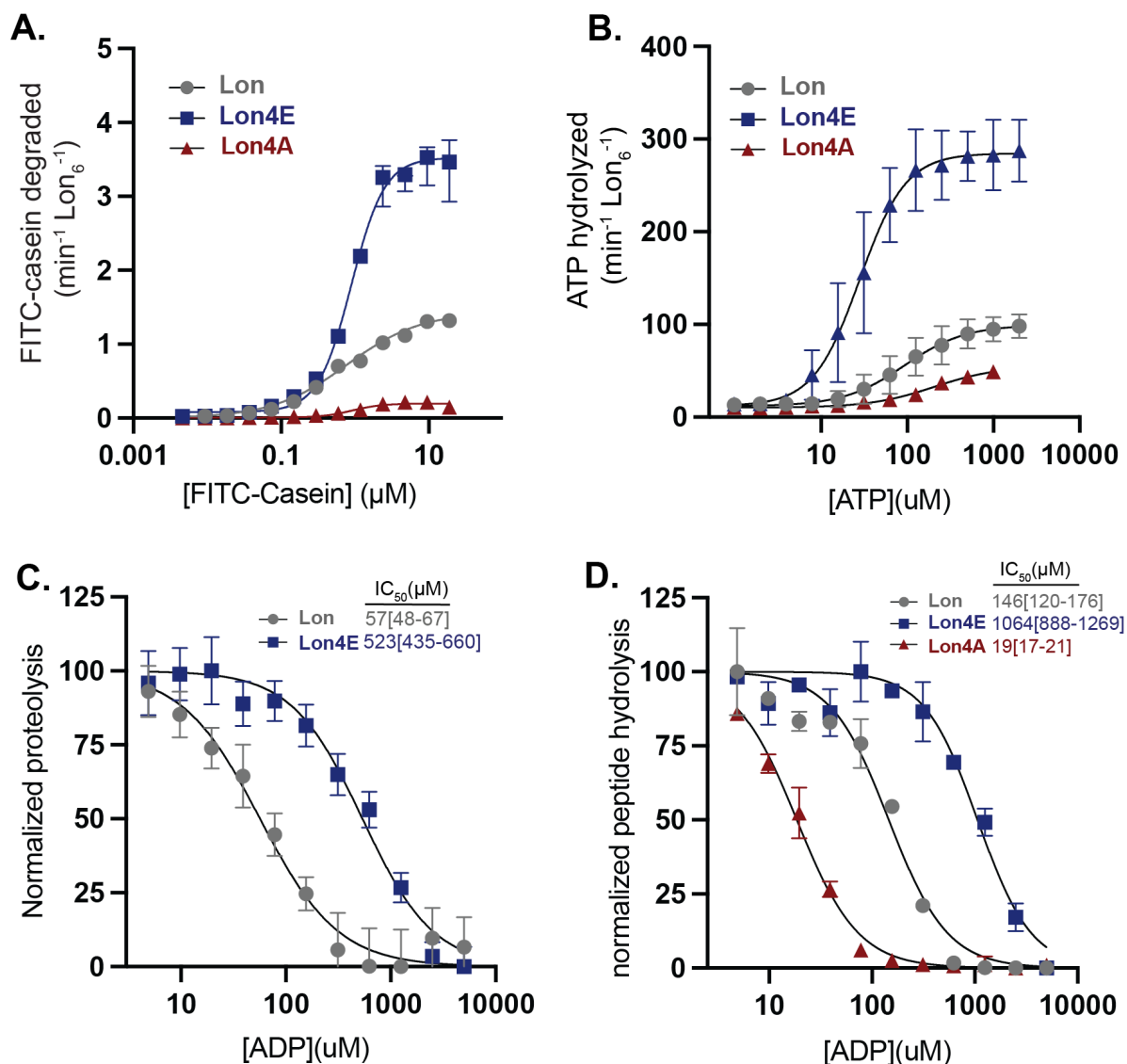
575

576

Figure 3



577
578 **Figure 3 Mutations in the Lon DNA binding site alter activity.** A. The following mutations
579 K301E/A, K303E/A, K305E/A and K306E/A were introduced in the DNA binding site of Lon. Dual
580 *in vitro* degradation and ATP hydrolysis were monitored with FITC and NADH as fluorescent
581 readouts of proteolysis and ATPase activity. B. *In vitro* gel based degradation assay of DnaA by
582 Lon alleles using an ATP regeneration mix and 5 μM DnaA. C. Peptide hydrolysis assays with
583 125 μM fluoro-peptide (described in Figure 1), 125 $\mu\text{g/mL}$ Casein and the ATP regeneration mix.
584
585

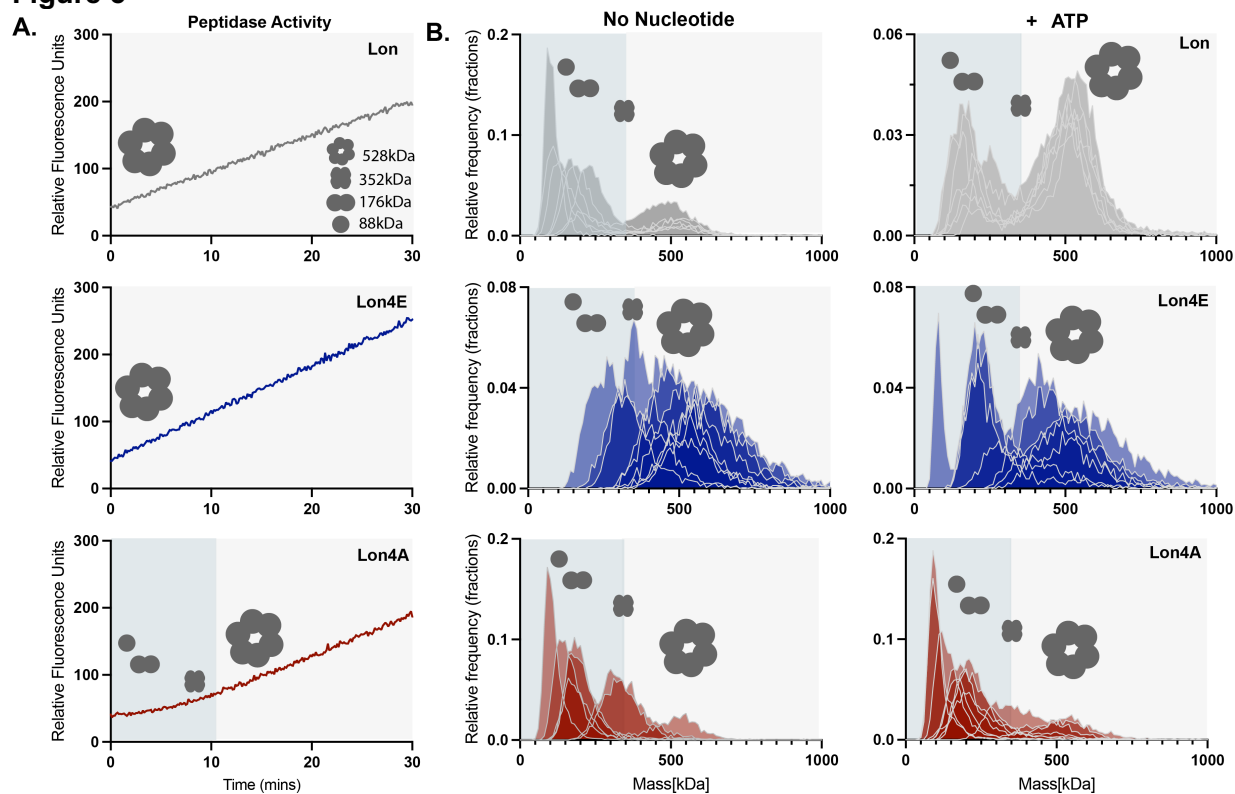


586
587
588
589
590
591
592
593
594
595
596
597
598
599
600
601
602
603

Figure 4 Negative surface charge at the DNA binding site of Lon increases nucleotide affinity. A. Degradation rates as a function of FITC-Casein concentration plotted using Michaelis-Menten kinetics. B. ATP hydrolysis as a function of ATP concentration. C. Normalized proteolysis as a function of ADP concentration to determine IC_{50} . D. Normalized peptide hydrolysis (as described in Figure 1) as a function of ADP concentration to measure IC_{50} . Experiments were performed in triplicate with the 95%CI reported.

604
605
606

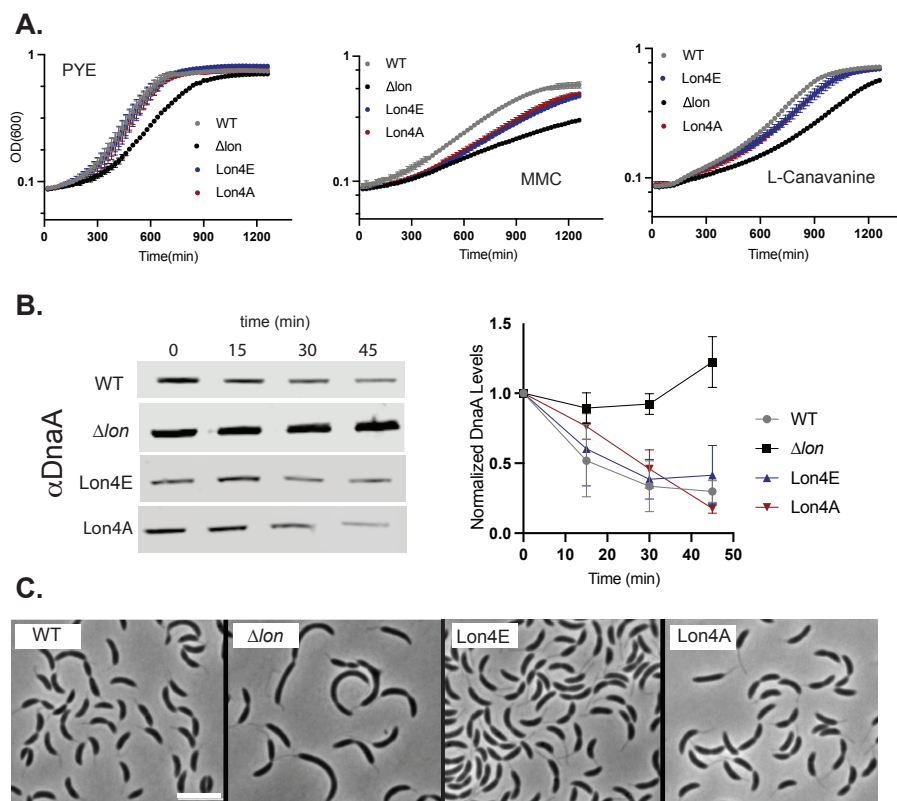
Figure 5



607
608
609
610
611
612
613
614
615
616
617
618

Figure 5. Charge state at the DNA binding site alters oligomerization. A. Peptide hydrolysis by Lon (100nM₆) variants with an ATP regeneration mix and 125 µg/mL casein (Inset displays predicted mass of Lon oligomers). B. Mass photometry analysis of Lon variants (200 nM monomer concentration) after diluting into TK buffer and after adding saturating ATP (1 mM). Density is plotted as a relative frequency against mass (kDa) with the relative kDa for each condition. Multiple replicates for each condition (n=7) are shown.

Figure 6



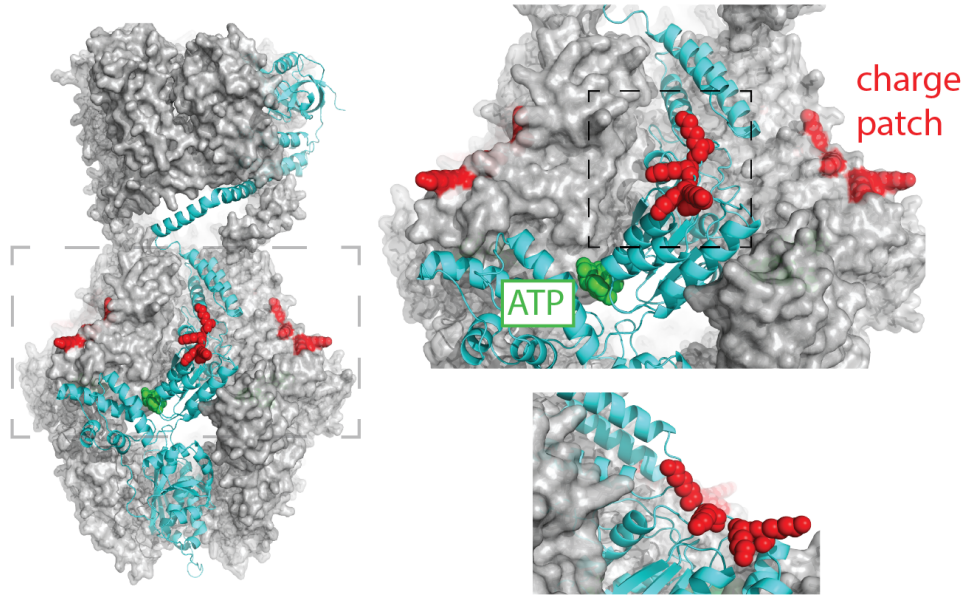
619
620
621
622
623
624
625
626
627
628
629
630

Figure 6. Lon alleles complement normal function with the exception of genotoxic stress.
A. 24-hour growth curve of Lon variants in normal growth conditions (PYE), with genotoxic stress (0.5 μ g/mL mitomycin C, MMC) and proteotoxic stress (100 μ g/mL L-canavanine). B. Translational shutoff assays to monitor DnaA stability in cell. Chloramphenicol was added to stop protein synthesis and lysates were taken at the time points specified using western blot analysis with a DnaA antibody. Quantifications of six individual replicates are shown; DnaA levels are normalized to ClpP. Error bars represent SD. C. Phase contrast microscopy of exponentially growing cells, scale bar is 5 microns.

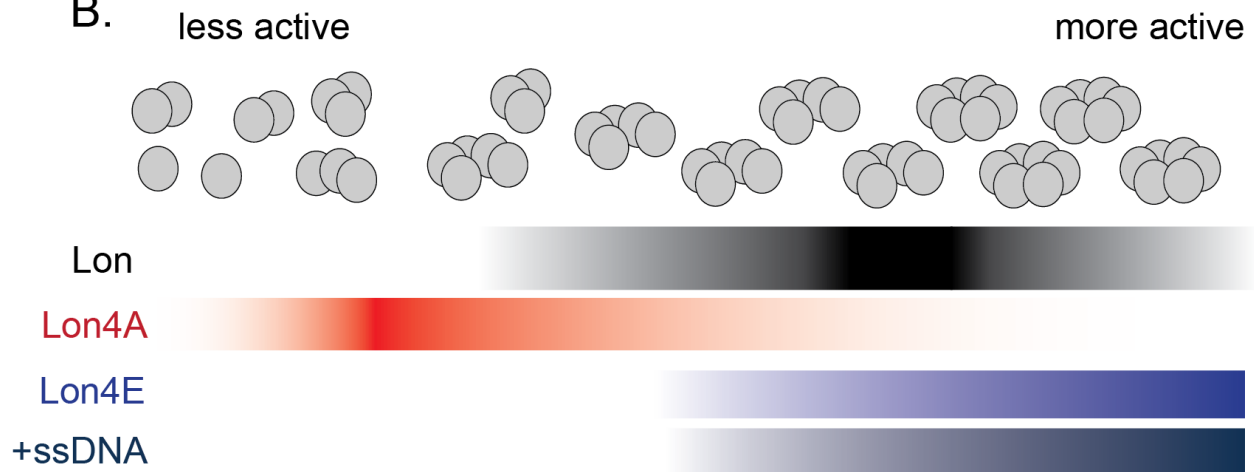
631
632
633
634

Figure 7

A.



B.

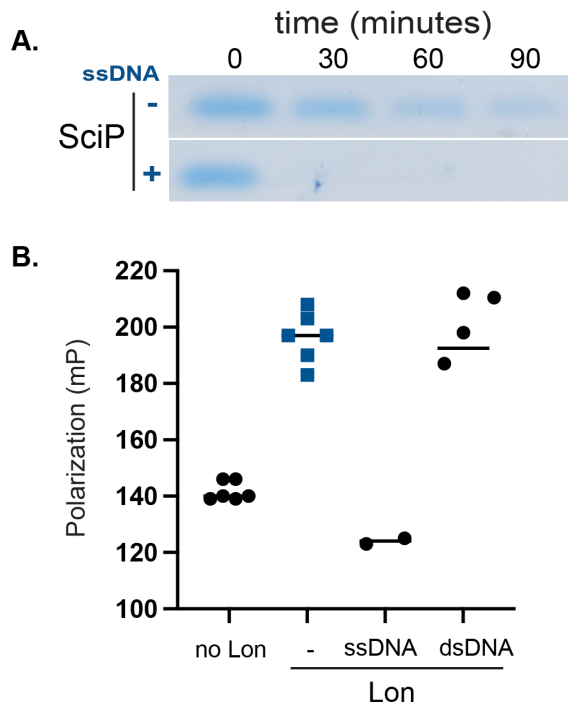


635
636
637
638
639
640
641
642
643
644
645
646
647

Figure 7. Lon activation and oligomerization are allosterically regulated by charge state at the DNA-binding sites. A. Structure of *Caulobacter* Lon as predicted by AlphaFold3. The inset displays the ATPase domain with DNA-binding residues in red (charge patch). A single monomer of the hexameric oligomer is highlighted (cyan) illustrating that the protomer-protomer interface residues responsible for ATP binding and hydrolysis (Walker A and B motif) are well-removed from the DNA-binding sites. B. Activity and oligomeric conformations of Lon depend on the overall electrostatics of the charge patch. Lon variants with negative residues at that site (Lon4E) or bound to DNA (+ssDNA) primarily form higher molecular weight oligomers. Neutralization of charge results in smaller, lower molecular weight complexes. Wildtype Lon can adopt a range of states depending on nucleotide, substrate, and effector binding.

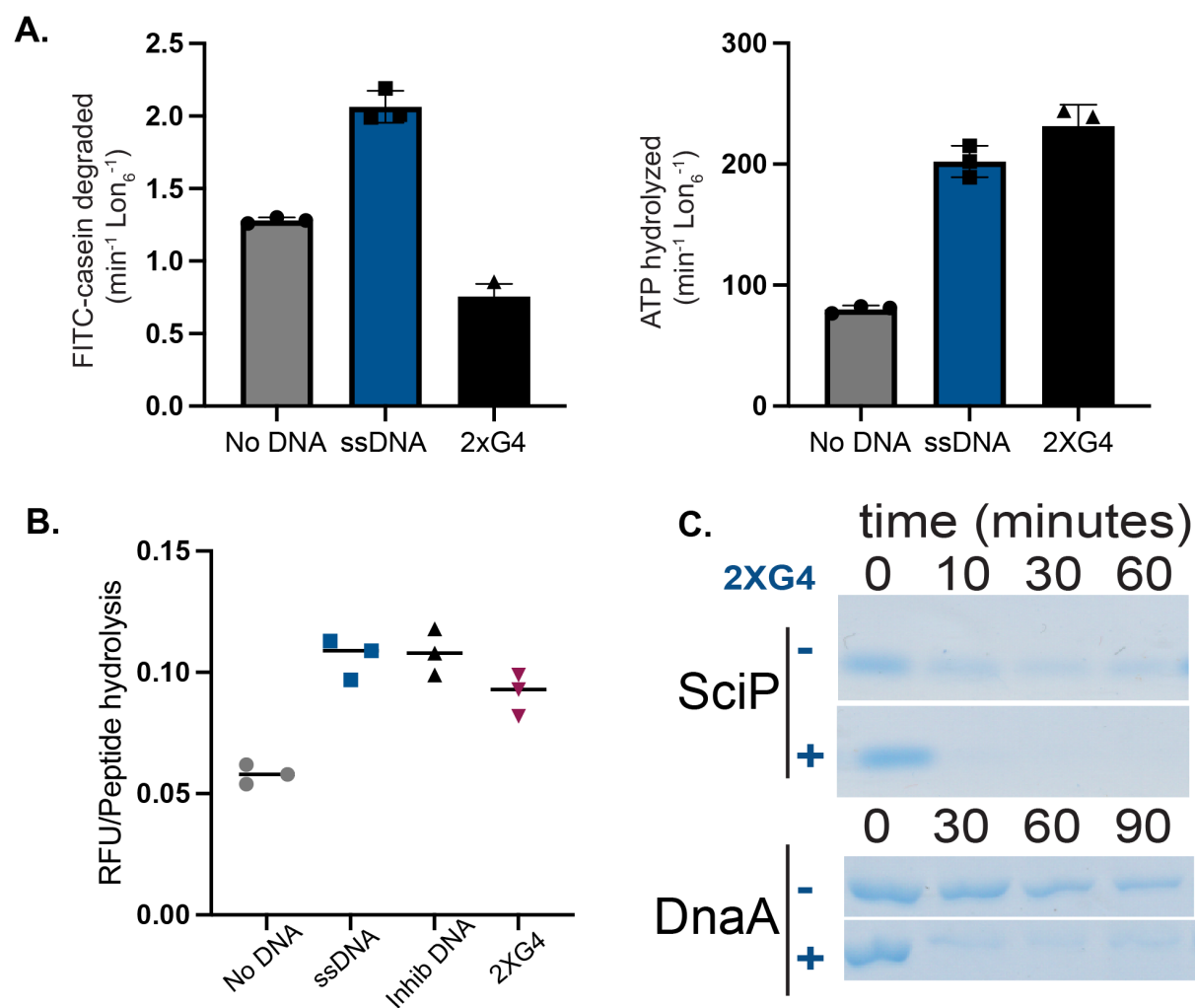
648
649
650

Supporting Information for Ogdahl and Chien



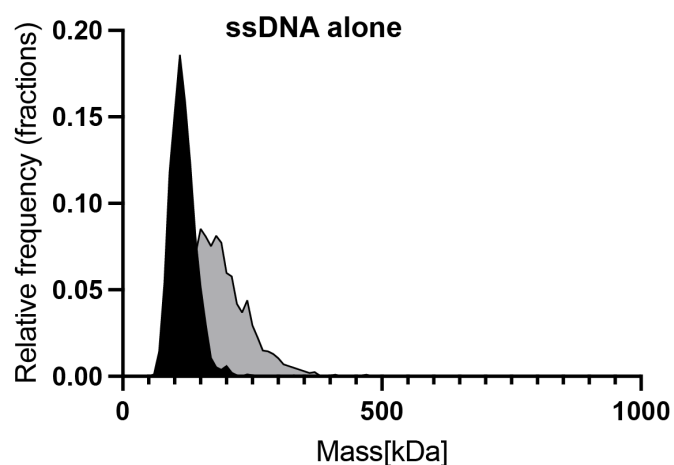
651
652
653
654
655
656
657
658

Supporting information Figure 1. A. *In vitro* degradation of SciP by Lon with and without ssDNA. Assay was performed using 0.1 μ M Lon, 20 μ M ssDNA and 5 μ M SciP. **B.** Fluorescent polarization assays using FAM-ssDNA and competing non-fluorescent ssDNA and dsDNA. Lon (0.1 μ M) measured with 25nM ssDNA.



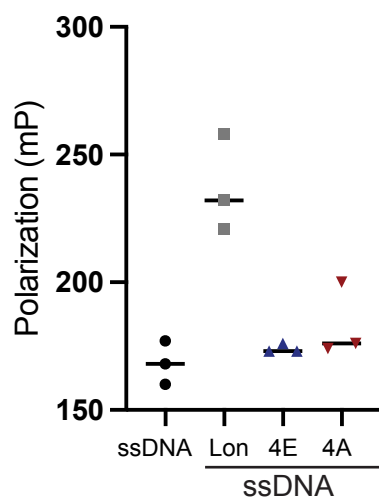
659
660
661
662
663
664
665
666
667
668

Supporting Information Figure 2. A. *In vitro* degradation and ATP hydrolysis assays using ssDNA with and without ssDNA containing 2 G4 DNA sequences (2XG4) inserted n=3. B. Peptide hydrolysis by Lon alone or with various ssDNA species (Inhib DNA contains two G quadruplexes) n=3. C. Gel based *in vitro* degradation of SciP (5 μ M) and DnaA (5 μ M) by 2XG4 ssDNA(20 μ M) (assay described in Figure 1).



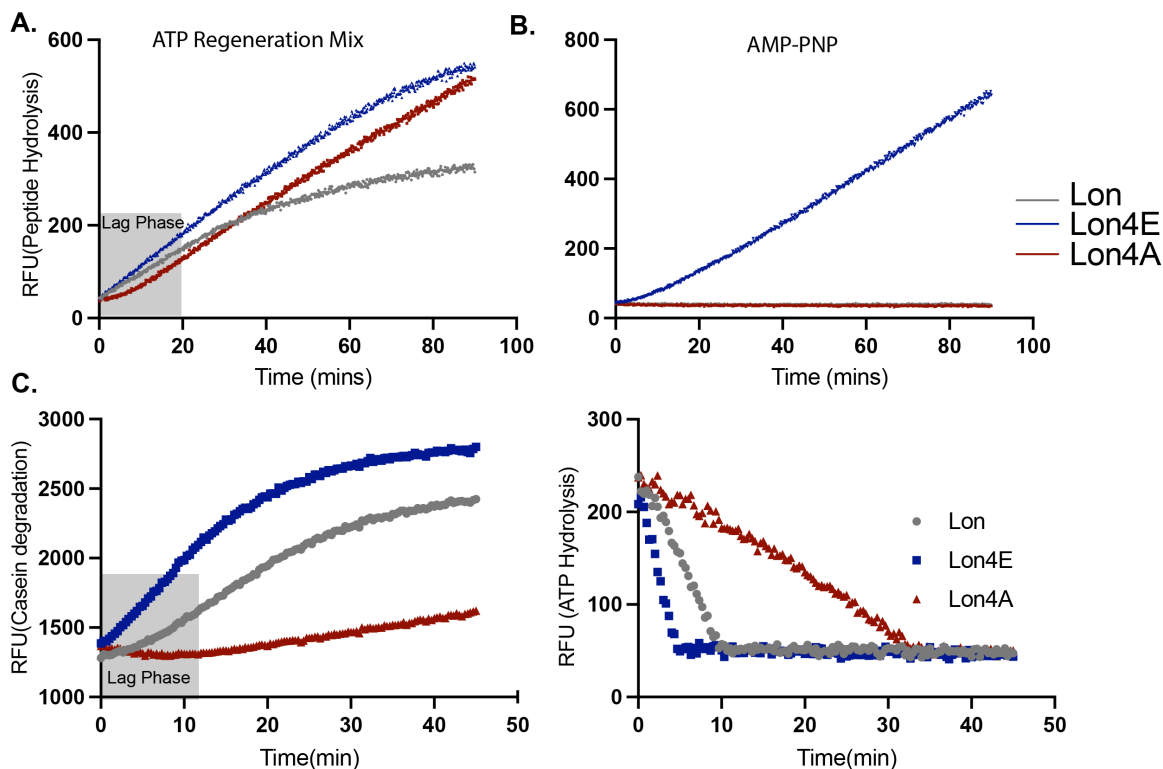
669
670 **Supporting Information Figure 3. ssDNA alone does not show high molecular weight**
671 **species.** Mass photometry of ssDNA (20 μ M) alone (described in Figure 2).
672

673
674
675
676
677
678
679
680
681
682
683
684
685
686
687
688
689
690



691
692 **Supporting Information Figure 4. Lon4E and Lon4A do not bind to DNA.** Fluorescent
693 polarization with FAM-ssDNA and Lon variants. 0.1 μ M Lon variant measured with 25nM ssDNA.
694 n=3
695

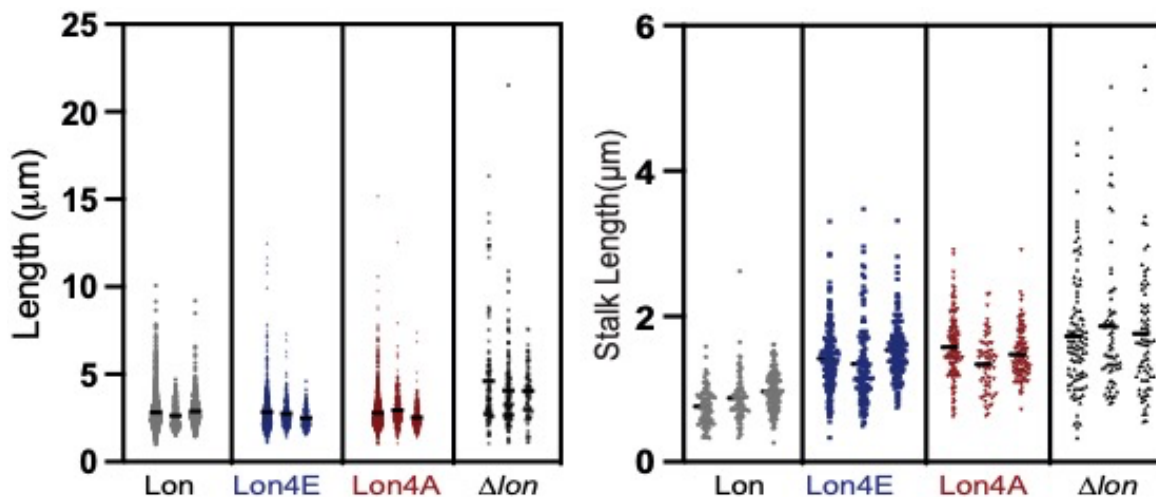
696
697
698



699

700 **Supporting Information Figure 5. All Lon alleles hydrolyze peptides with substrate and ATP,**
 701 **but the Lon4A has a lag period for all activity.** A. Peptide hydrolysis by Lon variants of 125 μ M
 702 fluor-peptide (described in Figure 1) and an ATP regeneration mix, 2mM ATP, Creatine Kinase,
 703 Creatine phosphate and casein. B. Peptide hydrolysis of 125 μ M peptide with 1mM AMP-PNP, a
 704 slow hydrolyzing analogue of ATP, and casein. C. Raw curves of *in vitro* proteolysis and ATP
 705 hydrolysis by Lon variants. Grey box defines the lag phase for Lon4A during peptide hydrolysis
 706 and proteolysis.

707
 708
 709



710

711 **Supporting Information Figure 6. Lon4E and Lon4A have similar cell lengths but exhibit**
 712 **longer stalks.** Cell length (MicrobeJ, Fiji) and stalk length measurements (Fiji) of the Lon alleles
 713 (representative cells shown in Figure 6) n=3.

714
 715
 716
 717
 718
 719

Supplemental Table 1. Plasmids and cell strains used in this study.

Plasmid or strain	Relevant characteristics	Comments	Reference
CPC176	Wild type strain	NA1000	
CPC667	Δlon	Clean delete	Lab collection
CPC741	Lon4E	Allele replacement pNPTS-138 plasmid	(24)
CPC1278	Lon4A	Allele replacement pNPTS-138 plasmid for Lon4A strain	This study
CPC605	lon::specR		(43)
EPC517	pET23b-His ₆ sumo-DnaA	BL21(DE3) Carb	(7)
EPC446	pET23b-His ₆ sumo-CcrM	BI21(DE3) Ampicillin	Lab collection
EPC565	375 SciP	BI21(DE3) Ampicillin	Lab collection
EPC460	pBAD33-Lon	BL21(DE3) Chloramphenicol	Lab collection
EPC1504	pBAD33-Lon4E	Top10 Chloramphenicol	(24)
EPC1796	pBAD33-Lon4A	BL21(DE3) Chloramphenicol	This study

720
 721
 722
 723
 724
 725
 726
 727
 728
 729
 730
 731

Supporting InformationTable 2. DNA sequences used in this study.

Name	DNA Sequence
OPC698-Stim	5'TCGATTCTCGAGTTAGTCGTCTTCTGGTGCCGGAAA3'
OPC498-Inhib	TGGGGTTAACGCTCTGTTAATCATGGGGAT
OJO19 (2XG4)	TCGGGGCTCGAGTTAGTCGTCTTCTGGTGGGGGAAA

FAM-ssDNA	FAM- AACGGATGATCCACAGGAGAGTCTGGCGCAGGGCGAGAG
G1Box	AACGGATGATCCACAGGAGAGTCTGGCGCAGGGCGAGAG
G1Box Reverse complement	CTCTCGCCCTGCGCCAGACTCTCCTGTGGATCATCCGTT
Lon4A_pNPTS	ACCGCAGCCATCGACCTCGTCGAGAGCGA
Lon4A_pNPTS	TGCGGCAGCGCCCCACGGGATCGACAGCAG
Lon4A_pBAD	ATCCCGTG GGGCGCTGCCGCAACCGCAGCCATCGACCTCG
Lon4A_pBAD	CGAGGTGATGGCTGCGGTTGCGGCAGCGCCCCACGGGAT

732
733
734
735
736
737
738
739
740
741
742
743